

## Charged magnons in $\alpha'$ -NaV<sub>2</sub>O<sub>5</sub>

A. Damascelli, D. van der Marel, M. Grüninger, C. Presura, and T.T.M. Palstra  
*Material Science Center, University of Groningen, Nijenborgh 4, 9747 AG Groningen, The Netherlands*

J. Jegoudez, and A. Revcolevschi  
*Laboratoire de Chimie des Solides, Université de Paris-sud, Bâtiment 414, F-91405 Orsay, France*  
 (10 March 1998)

We investigated the temperature-dependent optical conductivity of  $\alpha'$ -NaV<sub>2</sub>O<sub>5</sub> in the energy range 4 meV-4 eV. The intensities and the polarization dependence of the detected electronic excitations give a direct indication for a broken-parity electronic ground-state and for a non-centrosymmetric crystal structure of the system in the high-temperature phase. A direct two-magnon optical absorption process, proposed in this Letter, is in quantitative agreement with the optical data. By analyzing the optically allowed phonons at various temperatures above and below the phase transition, we conclude that a second-order change to a larger unit cell takes place below 34 K.

CuGeO<sub>3</sub> and  $\alpha'$ -NaV<sub>2</sub>O<sub>5</sub> are both insulating compounds exhibiting a temperature dependence of the magnetic susceptibility which has been discussed in terms of the one-dimensional (1D) S=1/2-Heisenberg spin chain. Moreover, a phase transition has been observed, at 14 K for CuGeO<sub>3</sub> [1] and at 34 K for  $\alpha'$ -NaV<sub>2</sub>O<sub>5</sub> [2], which is characterized by the opening of a spin gap and by superlattice reflections [3,4]. Together these observations have been interpreted as indications of a spin-Peierls (SP) phase transition. For both compounds, and in particular for CuGeO<sub>3</sub>, the 2D character can not be neglected and is the subject of intensive investigations. In this Letter we demonstrate that, in contrast with the situation in conventional SP systems, the low-energy spin excitations of  $\alpha'$ -NaV<sub>2</sub>O<sub>5</sub> carry a finite electric dipole moment. We probe this dipole moment directly in our optical experiments, and use it to measure the spin-correlations as a function of temperature.

The basic building blocks of the crystal structure of  $\alpha'$ -NaV<sub>2</sub>O<sub>5</sub> are linear chains of alternating V and O ions, oriented along the *b* axis [5]. These chains are grouped into sets of two, forming a ladder, with the rungs oriented along the *a* axis (see Fig. 1). The rungs are formed by two V ions, one on each leg of the ladder, bridged by an O ion. The V-O distances along the rungs are shorter than along the legs, implying a stronger bonding along the rung. In the *a*-*b* plane the ladders are shifted half a period along the *b* axis relative to their neighbors.

The average charge of the V ions of +4.5 implies an occupation of the V 3d band of half an electron which, in principle, implies metallic behavior. Lattice deformations can however lift the degeneracy between the two V sites. The early X-ray diffraction (XRD) analysis of Carpy and Galy [5] indicated the non-centrosymmetric space group *P2<sub>1</sub>mn*. In this structure it is possible to identify well-distinct magnetic V<sup>4+</sup> (S=1/2) and non-magnetic V<sup>5+</sup> (S=0) chains running along the *b* axis of the crystal and

alternating each other along the *a* axis. This configuration would be responsible for the 1D character of the high temperature susceptibility [6] and for the SP transition, possibly involving dimerization within the V<sup>4+</sup> chains [2]. The insulating character of  $\alpha'$ -NaV<sub>2</sub>O<sub>5</sub> would be an obvious consequence of having a 1D 1/2-filled Mott-Hubbard system. Recently, this structural analysis has been questioned and the centrosymmetric space group *Pmmn* was proposed [7,8]. In this context, it is still possible to recover an insulating ground state assuming that the *d* electron, supplied by the two V ions forming a rung of the ladder, is not attached to a particular V site but is shared in a V-O-V molecular bonding orbital along the rung [8]. However, the debate on the appropriate space group and electronic ground-state for  $\alpha'$ -NaV<sub>2</sub>O<sub>5</sub> is still open. While single-crystal XRD refinements indicate an inversion center, small deviations in atomic positions up to 0.03 Å could not be excluded [7].

In this Letter we present an investigation of the temperature-dependent optical conductivity of pure

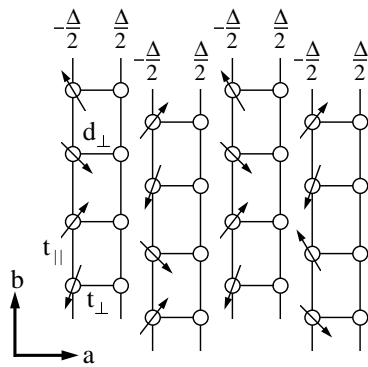


FIG. 1. Sketch of the ladder structure in the *a*-*b* plane of  $\alpha'$ -NaV<sub>2</sub>O<sub>5</sub>. The circles represent the V sites having on-site energies  $\pm\Delta/2$  on adjacent legs, alternatively. The arrows represent the electrons which are mainly distributed over legs characterized by lower potential energy for the V sites.

high-quality single crystals of  $\alpha'$ -NaV<sub>2</sub>O<sub>5</sub>. Based on our analysis of the charge-transfer (CT) absorption edge at 1 eV we provide strong support for a broken-parity ground-state of the quarter-filled ladder. This lack of inversion symmetry provides a mechanism for two-magnon optical absorption, and is shown to be in agreement with the observed oscillator strength and polarization dependence of the experimental data. Further experimental support for these 'charged magnons' is provided by the strong line-shape anomalies of the optical phonons.

High-quality single crystals of  $\alpha'$ -NaV<sub>2</sub>O<sub>5</sub> were grown by high temperature solution growth from a vanadate mixture flux. The crystals with dimensions of  $\sim 1 \times 3 \times 0.3$  mm<sup>3</sup> were aligned by Laue diffraction and mounted in a liquid He flow cryostat to study the temperature dependence of the normal incidence reflectivity between 30 and 30 000 cm<sup>-1</sup> in the temperature range 4-300 K. The optical conductivity was calculated from the reflectivity using Kramers-Kronig relations.

The *a* and *b*-axis reflectivity spectra at T=4 K and T=40 K are displayed in Fig. 2 up to 1000 cm<sup>-1</sup>, which covers the full phonon spectrum. In Fig. 3 we present the optical conductivity. The *b*-axis optical conductivity (along the chains) has no electronic absorption in the far infrared, which is characteristic of an insulating material. Along the *a* direction (along the rungs) we observe a broad band of weak optical absorption in the far and mid-infrared range. For both directions we observe a strong absorption at 8000 cm<sup>-1</sup> (1 eV), in agreement with Ref. 9. We observe 6 *a*-axis phonon modes at 90 (weak), 177, 372, 586, 740 (weak) and 938 cm<sup>-1</sup> (weak), and 4 *b*-axis modes at 137, 225 (weak), 256 and 518 cm<sup>-1</sup>. The factor group analysis gives 7 (15) *a*-axis and 4 (7) *b*-axis infrared active phonons for the *Pmmn* (*P2<sub>1</sub>mn*) space group. As some of the modes may have escaped detection (due to a small oscillator strength, to masking by the electronic infrared continuum or because the frequency is too low for our setup), neither of the two space groups can be ruled out on the basis of the number of experimentally observed phonons.

Let us now analyze the absorption band at 1 eV. An obvious candidate for such a strong optical transition is the on-rung CT involving the two V sites. We model the *j*-th rung with the Hamiltonian:

$$H_j = t_{\perp} \sum_{\sigma} \left\{ L_{j\sigma}^{\dagger} R_{j\sigma} + R_{j\sigma}^{\dagger} L_{j\sigma} \right\} + \Delta n_C + U \{ n_{jR\uparrow} n_{jR\downarrow} + n_{jL\uparrow} n_{jL\downarrow} \}, \quad (1)$$

where  $L_{j\sigma}^{\dagger}$  ( $R_{j\sigma}^{\dagger}$ ) creates an electron with spin  $\sigma$  on the left-hand (right-hand) V site of the *j*-th rung,  $U$  is the on-site Hubbard repulsion,  $t_{\perp}$  is the on-rung hopping parameter,  $n_C = \sum_j (n_{jR} - n_{jL})/2$  is the charge displacement operator, and  $\Delta$  is the potential energy difference between the two sites. For the symmetric ladder  $\Delta = 0$ . For a single electron per rung, the two solutions are lobe-sided bonding and anti-bonding combinations

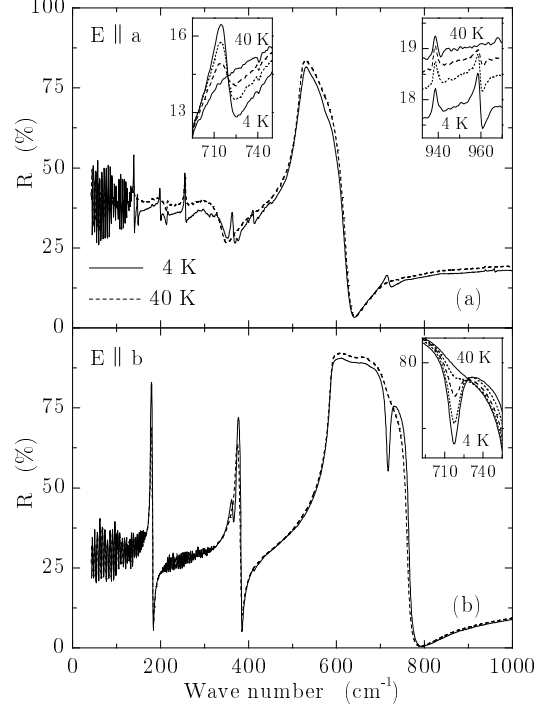


FIG. 2. Reflectivity spectra of  $\alpha'$ -NaV<sub>2</sub>O<sub>5</sub> for  $\vec{E} \parallel \vec{a}$  (a) and  $\vec{E} \parallel \vec{b}$  (b) below (4 K) and above (40 K) the phase transition. Insets: detailed temperature dependence of some of the new phonon lines detected for  $T < T_{SP}$ .

$|\tilde{L}\rangle = u|L\rangle + v|R\rangle$ , and  $|\tilde{R}\rangle = u|R\rangle - v|L\rangle$  where  $1/(2uv)^2 = 1 + (\Delta/2t_{\perp})^2$ . The splitting between these two eigenstates,  $E_{CT} = \sqrt{\Delta^2 + 4t_{\perp}^2}$ , corresponds to the photon energy of the optical absorption (1 eV).

A second crucial piece of information is provided by the intensity of the absorption. We use the following expression, which is exact for one electron on two coupled tight-binding orbitals [10]:

$$\int_{peak} \sigma_1(\omega) d\omega = \pi e^2 N d_{\perp}^2 t_{\perp}^2 \hbar^{-2} E_{CT}^{-1}, \quad (2)$$

where  $N$  is the volume density of the rungs and  $d_{\perp} = 3.44$  Å is the distance between the two V ions on the same rung (see Fig. 1). This way we calculated from the spectra  $|t_{\perp}| \approx 0.3$  eV. Combining this number with  $E_{CT} = 1$  eV we obtain  $\Delta \approx 0.8$  eV. The corresponding two eigenstates have 90 % and 10 % character on either side of the rung. Therefore the valence of the two V-ions is 4.1 and 4.9, respectively. The optical transition at 1 eV is essentially a CT excitation from the occupied V 3d state at one side of the rung to the empty 3d state at the opposite side of the same rung.

Let us now turn to the infrared continuum for  $\vec{E} \parallel \vec{a}$  [an enlarged view is given in inset (a) of Fig. 3]. As the range of frequencies coincides with the low energy-scale spin excitations, the most likely candidates for this continuum are excitations involving two spin flips. Another reason for this assignment is the opening, for  $T < T_{SP}$  [11],

of a gap in the optical conductivity of  $17 \pm 3$  meV (*i.e.*, approximately twice the spin gap value [4,12]). The presence of *two* V states ( $|L\rangle$  and  $|R\rangle$ ) per spin, along with the broken left-right parity of the ground state, gives rise to a fascinating behavior of the spin flips: Consider a small fragment of the ladder with only two rungs, with one spin per rung. Each rung is described by the Hamiltonian defined above. In the ground state of this cluster each spin resides in a  $|L\rangle$  orbital, with some admixture of  $|R\rangle$ . Let us now include the coupling of the two rungs along the legs, using:

$$t_{\parallel} \sum_{\sigma} \left\{ R_{1,\sigma}^{\dagger} R_{2,\sigma} + L_{1,\sigma}^{\dagger} L_{2,\sigma} + H.C. \right\}. \quad (3)$$

If the two spins are parallel, the inclusion of this term has no effect, due to the Pauli-principle. If they form a  $S = 0$  state, the ground state can gain some kinetic energy along the legs by mixing in states where two electrons reside on the same rung. Working in the limit that  $U \rightarrow \infty$ , these states have one electron in the  $|L\rangle$  and one in the  $|R\rangle$  state on the same rung. As a result, there is a net dipole displacement of the singlet state compared to the triplet state: *The spin-flip excitations carry a finite electric dipole moment.* Using a perturbation expansion in  $t_{\parallel}/E_{CT}$ , and working in the limit  $U \rightarrow \infty$ , the exchange coupling constant between two spins on neighboring rungs becomes:

$$J_{\parallel} = \frac{8t_{\parallel}^2 t_{\perp}^2}{[\Delta^2 + 4t_{\perp}^2]^{3/2}}. \quad (4)$$

The coupling to infrared light with  $\vec{E} \parallel \vec{a}$  can now be included using the dipole approximation. The only effect is to change the potential energy of the  $|R\rangle$  states relative to the  $|L\rangle$  states. In other words, we have to replace  $\Delta$  with  $\Delta + q_e d_{\perp} E_a$ , where  $q_e$  is the electron charge, and  $E_a$  is the component of the electric field along the rung. By expanding  $J_{\parallel}$  we obtain the spin-photon coupling:

$$H_S = q_m d_{\perp} E_a h_S = q_m d_{\perp} E_a \sum_j \vec{S}_j \cdot \vec{S}_{j+1}, \quad (5)$$

where  $q_m = q_e \frac{3J_{\parallel}\Delta}{\Delta^2 + 4t_{\perp}^2}$  is the effective charge involved in a double spin-flip transition. For a symmetrical ladder, where  $\Delta = 0$ , the effective charge vanishes, and the charged magnon effect disappears. In that case higher-order processes like the phonon assisted spin-excitations, considered by Lorenzana and Sawatzky [13], can still contribute. These are probably responsible for the weak mid-infrared continuum in the  $\vec{E} \parallel \vec{b}$  spectra.

Taking the values of  $t_{\perp}$  and  $\Delta$  calculated from the optical data and  $|t_{\parallel}| \approx 0.2$  eV [14] we obtain  $J_{\parallel} \approx 30$  meV (comparable to the reported values ranging from 38 [12] to 48 meV [2]), and  $q_m/q_e = 0.07$ . Using the functions:

$$\begin{aligned} g_S(T) &\equiv 4 \langle\langle h_S^2 \rangle\rangle - \langle h_S \rangle^2 \rangle_T, \\ g_C(T) &\equiv 4 \langle\langle n_C^2 \rangle\rangle - \langle n_C \rangle^2 \rangle_T, \end{aligned} \quad (6)$$

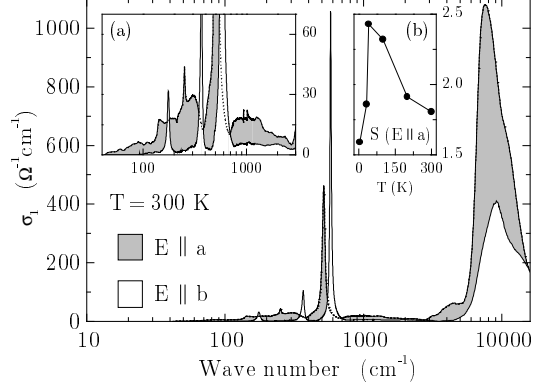


FIG. 3. Optical conductivity of  $\alpha'$ - $\text{NaV}_2\text{O}_5$  at 300 K for  $\vec{E} \parallel \vec{a}$  and  $\vec{E} \parallel \vec{b}$ . Inset (a): enlarged view of  $\sigma_1(\omega)$  from 40 to  $3000 \text{ cm}^{-1}$ . Inset (b): oscillator strength of the electronic continuum for  $\vec{E} \parallel \vec{a}$  plotted versus temperature.

we can express the intensity of the spin-fluctuations relative to the CT excitations in terms of the effective charge:

$$\frac{\int_S \sigma_1(\omega) d\omega}{\int_{CT} \sigma_1(\omega) d\omega} = \frac{q_m^2 g_S E_S}{q_e^2 g_C E_{CT}}. \quad (7)$$

It is easy to prove that  $g_C = (2uv)^2$ . For the present parameters,  $g_C \simeq 0.4$ .  $E_S$  is the average energy of the infrared spin fluctuation spectrum and is of the order of 0.1 eV. The spin-correlation function  $g_S$  depends on the details of the many-body wave function of the spins. For an antiferromagnetic chain  $g_S = 1$ , whereas for a random orientation of the spins it is zero. In between it depends on the probability of having fragments of three neighboring spins ordered antiferromagnetically. Hence the maximum relative intensity in Eq. (7) is  $\sim 0.0014$ . The experimental value is  $\sim 0.0008$  at  $T=300$  K, in good agreement with the numerical estimate. Note, that a finite value of  $g_S$  requires either terms in the Hamiltonian which do not commute with  $h_S$ , or an antiferromagnetic broken symmetry of the ground state.

Remarkable is also the temperature dependence of the spin-fluctuation continuum observed for  $\vec{E} \parallel \vec{a}$ . The oscillator strength, obtained by integrating  $\sigma_1(\omega)$  (with phonons subtracted) up to  $800 \text{ cm}^{-1}$ , is displayed in inset (b) of Fig. 3. It increases upon cooling down the sample from room temperature to  $T_{SP}$  and rapidly decreases for  $T < T_{SP}$ . Within the discussion given above, this increase marks an increase in short range antiferromagnetic correlations of the chains. Below the phase transition, nearest neighbor spin-singlet correlations become dominant, and  $g_S$  is suppressed.

Upon cooling down the sample below  $T_{SP}=34$  K, significant changes occur in the phonon spectrum (see Fig. 2). Contrary to  $\text{CuGeO}_3$  [15], where we observed in reflectivity a single, very weak additional phonon, 10 new lines are detected for  $\vec{E} \parallel \vec{a}$  ( $\omega_{TO} \approx 101, 127, 147, 199, 362, 374, 410, 450, 717$ , and  $960 \text{ cm}^{-1}$ ), and 7 for  $\vec{E} \parallel \vec{b}$  ( $\omega_{TO} \approx 102, 128, 234, 362, 410, 718$ , and  $960 \text{ cm}^{-1}$ ), some of them

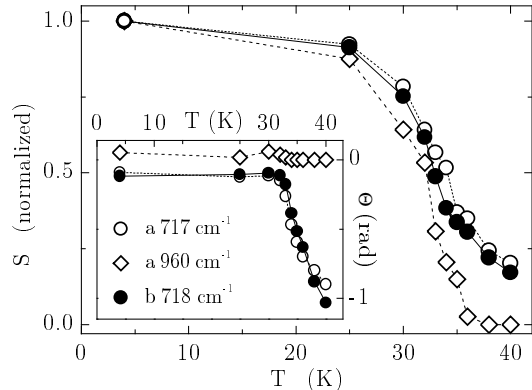


FIG. 4. Temperature dependence of the normalized oscillator strength of the zone boundary modes observed at 717 and 960  $\text{cm}^{-1}$ , for  $\vec{E} \parallel \vec{a}$ , and at 718  $\text{cm}^{-1}$ , for  $\vec{E} \parallel \vec{b}$ . Inset: Fano asymmetry parameter for these lines.

showing a quite large oscillator strength. An enlarged view of few of these phonons is given in the insets of Fig. 2. The observation of almost the same frequencies for both axes, which is an important information for a full understanding of the structural distortion, is an intrinsic property of the low temperature phase. Experimental errors, like polarization leakage or sample misalignment, are excluded from the well-defined anisotropic phonon spectrum of the undistorted phase. The larger intensity of the lines, with respect to the case of  $\text{CuGeO}_3$  [15], reflects the larger lattice distortions in  $\alpha'\text{-NaV}_2\text{O}_5$  on going through the phase transition. At the same time the strong line-shape anomalies of all infrared active phonons for  $\vec{E} \parallel \vec{a}$  indicate a strong coupling to the spin-fluctuation continuum. We like to speculate here that this is due to coupling of the phonons to the electric dipole moment of the charged magnons.

We carefully investigated the activated modes at  $\approx 718$  and  $960 \text{ cm}^{-1}$ , at temperatures ranging from 4 to 40 K. We fitted these phonons to a Fano profile because the  $718 \text{ cm}^{-1}$  modes show an asymmetrical line-shape. The results of the normalized oscillator strength  $S$  are plotted versus temperature in Fig. 4. In the inset we also present the asymmetry parameter  $\Theta$ , defined in such a way that for  $\Theta=0$  a Lorentz line-shape is recovered [16].  $S$  has a similar behavior for the three different lines. However, the  $960 \text{ cm}^{-1}$  peak vanishes at  $T_{\text{SP}}$  whereas the two  $718 \text{ cm}^{-1}$  modes have still a finite intensity at  $T=40 \text{ K}$  and, as a matter of fact, disappear only for  $T>60\text{-}70 \text{ K}$ . At the same time, the line-shape of the  $960 \text{ cm}^{-1}$  mode is perfectly lorentzian at all temperatures, whereas the two other phonons show a consistently increasing asymmetry for  $T>32 \text{ K}$ . From these results we conclude that the second-order character of the phase transition is nicely shown by the behavior of  $S$  for the  $960 \text{ cm}^{-1}$  folded mode. On the other hand, pretransitional fluctuations manifest themselves in the finite intensity of the  $718 \text{ cm}^{-1}$  modes above  $T_{\text{SP}}$ . Similar pretransitional fluctuations have been observed below 70 K in the course of a study

of the propagation of ultrasonic waves along the chain direction of  $\alpha'\text{-NaV}_2\text{O}_5$  [17].

In conclusion, by a detailed analysis of the optical conductivity we provide direct evidence for the broken-parity electronic ground-state and for the non-centrosymmetric crystal structure of the high temperature phase of  $\alpha'\text{-NaV}_2\text{O}_5$ . We show that a direct two-magnon optical absorption process is responsible for the low frequency continuum observed perpendicularly to the chains. By analyzing the optically allowed phonons at various temperatures, we conclude that a second-order change to a larger unit cell takes place below 34 K, with a fluctuation regime extending over a very broad temperature range.

We gratefully acknowledge A. Lande, M. Mostovoy, D.I. Khomskii, and G.A. Sawatzky for stimulating discussions. We thank D. Smirnov, J. Leotin, M. Fischer and P.H.M. van Loosdrecht for many useful comments, and C. Bos, A. Meetsma and J.L. de Boer for assistance. This investigation was supported by the Netherlands Foundation for Fundamental Research on Matter (FOM) with financial aid from the Nederlandse Organisatie voor Wetenschappelijk Onderzoek (NWO).

---

- [1] M. Hase, I. Terasaki, and K. Uchinokura, Phys. Rev. Lett. **70**, 3651 (1993).
- [2] M. Isobe, and Y. Ueda, J. Phys. Soc. Jpn. **65**, 1178 (1996).
- [3] J.P. Boucher, and L.P. Regnault, J. Phys. I France **6**, 1939 (1996).
- [4] Y. Fujii, *et al.*, J. Phys. Soc. Jpn. **66**, 326 (1997).
- [5] P.A. Carpy, and J. Galy, Acta Cryst. B **31**, 1481 (1975).
- [6] F. Mila, P. Millet, and J. Bonvoisin, Phys. Rev. B. **54**, 11 925 (1996).
- [7] A. Meetsma, *et al.*, submitted to Acta Cryst..
- [8] H. Smolinski, *et al.*, cond-mat/9801276.
- [9] A. Golubchik, *et al.*, J. Phys. Soc. Jpn. **66**, 4042 (1997).
- [10] J.M. Ziman, *Principles of the Theory of Solids* (Cambridge University Press, Cambridge, 1972), p. 261, noticing that  $\langle 0 | x | CT \rangle = -d_{\perp} t_{\perp} / E_{CT}$ .
- [11] A. Damascelli, *et al.*, unpublished.
- [12] M. Weiden, *et al.*, Z. Phys. B **103**, 1 (1997).
- [13] J. Lorenzana, and G.A. Sawatzky, Phys. Rev. B **52**, 9576 (1995).
- [14] W.A. Harrison, *Electronic Structure and the Properties of Solids* (Dover Publications, New York, 1989).
- [15] A. Damascelli, *et al.*, Phys. Rev. B. **56**, R11373 (1997); Physica B **244**, 114 (1998).
- [16] A. Damascelli, *et al.*, Phys. Rev. B. **55**, R4863 (1997).
- [17] P. Fertey, *et al.*, to be published in Phys. Rev. B.